

# We are IntechOpen, the world's leading publisher of Open Access books Built by scientists, for scientists

4,800

Open access books available

122,000

International authors and editors

135M

Downloads

Our authors are among the

154

Countries delivered to

TOP 1%

most cited scientists

12.2%

Contributors from top 500 universities



WEB OF SCIENCE™

Selection of our books indexed in the Book Citation Index  
in Web of Science™ Core Collection (BKCI)

Interested in publishing with us?  
Contact [book.department@intechopen.com](mailto:book.department@intechopen.com)

Numbers displayed above are based on latest data collected.  
For more information visit [www.intechopen.com](http://www.intechopen.com)



---

# Micromechanical Behavior of CuAlBe Shape Memory Alloy Undergoing 3-Point Bending Analyzed by Digital Image Correlation

---

R.J. Martínez-Fuentes, F.M. Sánchez-Arévalo, F.N. García-Castillo,  
G.A. Lara-Rodríguez, J. Cortés-Pérez, A. Reyes-Solís

Additional information is available at the end of the chapter

<http://dx.doi.org/10.5772/48772>

---

## 1. Introduction

The study and development of new materials have been used to forge new technology. Shape memory alloys (SMA's) have been cataloged as new materials which applications are in fields like the construction industry where these materials have been used as mechanical elements of damping; in medicine, SMA's have been used for biomechanical prosthesis in order to correct the position of bones and also to make surgical instruments. In these applications, because of their mechanical behavior, SMA's can substitute more efficiently, conventional materials. To get a better understanding of SMA's, new investigations are needed.

In recent years, the scientific and technologic community has been interested in the study of "exotic materials" like shape memory alloys (SMA's). Shape memory alloys are materials that can recover their original shape, after being elastically or pseudo-plastically deformed, by increasing their temperature; all these associated to a martensitic transformation [1,2]. The martensitic transformation is defined as a first-order displacive process, where a body center cubic parent phase (austenitic phase) transforms by a shearing mechanism into a monoclinic or orthorhombic martensitic phase [1]. The shape memory effects are useful in replacing conventional materials and developing new applications in science and industry. The SMA's present some associated effects like single, double shape memory effects and superelastic effect. All these effects are well known and they have been reported in literature for several authors [3-7].

The superelastic effect is one of the reasons that have encourage a continuous effort to understand, predict and explore the shape memory behavior of these materials. Since the

CuAlBe system appeared in 1982; it is considered one of the first studies that were done in Cu-Al-Be shape memory alloys by Higuchi et al. These works studied the influence of the thermal stability of Cu-Al-Be alloy which had a nearly eutectoid composition; Higuchi et al. observed small changes in the temperatures of transformation and also realized that the austenite phase was not decomposed up to 300 °C. With the thermal cycling also were observed the displacement variations; this was confirmed with a coil with a constant load; increasing the coil temperature, small displacement were register; thus the two way shape memory effect was reported in Cu-Al-Be [8,9].

After a while other interesting works concerning with this alloy were developed. Belkahla et al. reported the elaboration and characterization of a low temperature of the Cu-Al-Be shape memory alloy; obviously this work was based in Higuchi's research. The main contributions of this work were the quasi-binary Cu-Al phase diagram with the addition of 0.47 wt.% of beryllium and the  $M_s$  analytical expression, as a function of elements composition, to determine the critical temperature that indicates the start of the martensitic transformation. This study confirmed that the addition of small concentration of beryllium Cu-Al system decreased the eutectoidal temperature around 50 °C. In addition to the temperature decrement, a new ternary domain was observed; here the phase  $\alpha$ ,  $\beta$  and  $\gamma_2$  are present [10].

Jurado et al. were concerned about the order-disorder phase transition in Cu-Al-Be system alloys; in this case the studied ally was close to the eutectic composition. The main contribution of Jurado et al. was to reveal the effect of beryllium atom on the ordering behavior of the Cu-Al based alloys. Nowadays the X-Ray diffraction measurements reported by Jurado et al. are very useful to identify the involved phases in this system [11].

If order-disorder behavior takes place in CuAlBe system, it is obvious that this material can exhibit different mechanical response. The difference in mechanical behavior is due to the high anisotropy of this material. As a matter of fact, the Cu-Al-Be system presents three kinds of anisotropy. The first type is due to the austenitic phase and it is known as an inherent anisotropy. The second type is known as transformational anisotropy; this depends on the applied stress level or even the test temperature, preferential crystal orientation due to manufacturing process of the material. The last kind anisotropy is related with the mixture of austenite and martensite phases; the proportions of both phases, in the alloy, will change the mechanical response of this material. In order to clarify the mechanical response of this material some studies on the thermomechanical behavior has been done in monocrystals of Cu-Al-Be. These studies were able to determine the metastable phase stress vs. temperature diagram ( $\sigma$ -T). With this diagram is possible to get the critical stress or transformation stress value if the martensite phase is induced by stress [12].

Siredey and Eberhardt presented other interesting result, on the fatigue behavior of Cu-Al-Be monocrystals. A model to explain the fatigue mechanism was proposed. This model was based on the assumption that there are different zones where the martensite phase gets reordering or other diffusional phenomena, which vary the expected behavior inside the material; so the  $M_s$  temperature can change locally and it will modify the global behavior of

the material [13]. As it was previously mentioned the X-ray and differential screw calorimetric studies represent a suitable way to characterize shape memory materials. Balo et al. used these techniques to show the influence of heat treatments and beryllium content for this alloy. In this study can be observed the indexed X-ray pattern for martensite phase in addition the lattice parameters for 18R martensite were reported too [14,15].

All previous research has motivated the improvement of the Cu-Al-Be system in order to spread its application in different industry branches. One aspect to improve in this system is the mechanical properties that depend on the alloy's microstructure. In other words the involved phases and grain size have to be customized. In order to modify the mechanical response of Cu-A-Be system several grain refiners have been used. Ultrasonic and mechanical tensile testing has proved the influence of those refiners by different authors [16,17].

More specific studies, to understand the mechanical behavior of SMA, were done using non-conventional techniques to mimic the martensitic transformation in the superelastic regime for both monocrystal and polycrystal CuAlBe undergoing tension [18-20]. As a result, scientists have proposed transformation criterions, constitutive equations and also new tools to be familiar with the involve mechanisms during the martensitic transformation [21-26]. As it can be notice, considerable efforts have been done to understand the complex behavior of SMA's; mainly, because of their properties will eventually lead to replace conventional materials with these alloys.

Although there are several works trying to explain the mechanical behavior of SMA's nobody has studied the stress-induced martensitic transformation and its granular interaction in 2D-confined polycrystalline sample of CuAlBe undergoing 3-point bending by Digital Image Correlation. That is why the objective of this work is based on getting a practical methodology to understand the micro and macromechanical behavior of poly and monocrystalline Cu-Al 11.2 wt.%-Be 0.6 wt% , Cu-Al 11.2 wt.%-Be 0.5 wt% (respectively) undergoing a stress-induced martensitic transformation by a 3-point bending using digital image correlation.

Taking in to account the good thermal stability, excellent shape memory properties, temperature transformation wide ranges, damping capacity and low cost of production, the Cu-Al-Be system has become in a excellent alternative to take advantage of the shape memory effects; that is why several works will be conducted to get a full understanding on the Cu-Al-Be properties.

## 2. Experimental details

The experimental section describes the elaboration and characterization of the material. The first part of this section is focused in the elaboration and structural characterization of the material. The second part is dedicated to the mechanical arrangement that makes possible the simultaneous state of stress (tension and compression) in the sample.

## 2.1. Material

As it was previously mentioned, the composition was Cu-Al 11.2 wt%-Be 0.6 wt%, and Cu-Al 11.2 wt%-Be 0.5 wt% which is close to the eutectoidal composition [10]. An induction furnace (Leybold-Heraeus) was employed to elaborate the alloy by a melting process; this furnace has a controlled atmosphere and in our case argon gas was used. From the castings, suitable slices were cut and then hot rolled to obtain thin sheets. The length, width and thickness of the sheets were 280, 57 and 0.7-0.9 millimeters, respectively. These dimensions were reached after a 191 % hot-rolled (800 °C) deformation process. The hot-rolled process was carried out in an oven (Sola Basic-Lindberg model 847) and a roll machine (Fenn Amca International). Subsequently, the sheets were subjected to a heat treatment, called betatization, to reveal the shape memory effects; the sheets were heated at 750 °C during 15 minutes and then water-quenched to 95 °C during 20 minutes [24]. Then the samples were studied by X-ray diffraction (Bruker AXS modelo D8 Advance) in order to detect the phases involved in the alloy; finally Critical transformation temperatures were obtained by DSC 2910 Modulated de TA Instrument. After this, the sheets were cut in rectangular samples according to the beam theory.

## 2.2. Three-Point bending test

Bending tests were carried out on a servohydraulic loading device (MTS 858 MiniBionix axial). To acquire images an optical microscope was coupled to a CCD camera. The modular microscope works as an infinity-corrected compound microscope with magnifications of 2X. To control the MiniBionix MTS a 407 MTS controller was used while data and images acquisition were acquired by a National Instruments PXI-1002 chassis and PXI-boards (6281, 8331 and 1402) connected to a PC. White light illumination (150 W quartz halogen light source) was used to observe the microstructural behavior of the SMA under bending (see Fig. 1).

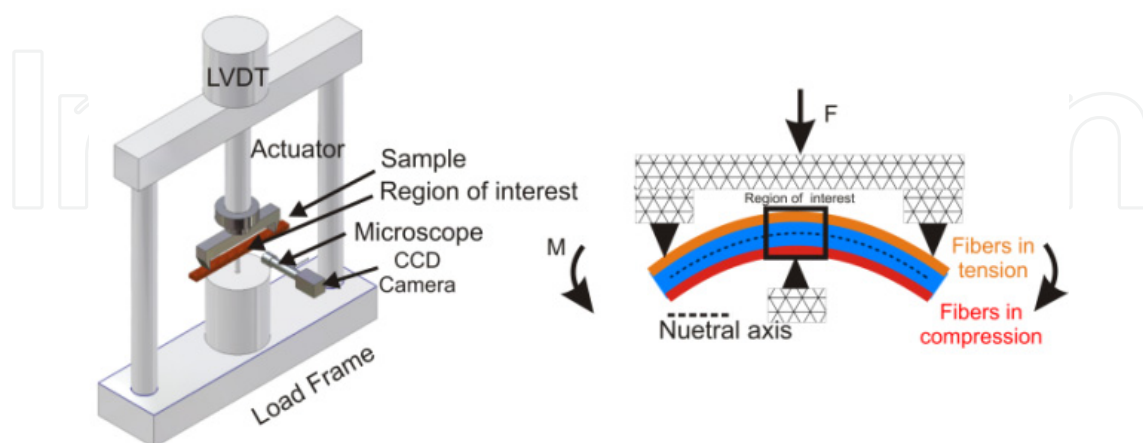


**Figure 1.** Experimental setup

In order to have a better understanding of CuAlBe mechanical behavior under bending a single-crystal of CuAlBe was also studied under the same conditions. Hence it was possible

to compare the mechanical behavior of monocrystalline and polycrystalline samples under bending. From the image sequence were determine the displacement vector fields at the region of interest, using digital image correlation, associated to bending test for both cases.

With the series of images acquired during the bending test, displacement vector fields were calculated from pairs of images. The Willert and Gharib algorithm [27] was used to calculate the displacement field  $u_k(x_k, y_k)$  and  $v_k(x_k, y_k)$ , where  $u$  and  $v$  represent the displacements of an analysis object or region of interest in the  $x$  and  $y$  directions respectively [28, 29]. The  $x$  and  $y$  represent the position coordinates of the analysis object in every image; subindex  $k$  indicates the corresponding object, which is defined as a 64x64 pixels subregion of interest. Hence was possible to observe the mechanical behavior in tension and compression by grain simultaneously.

### 3. Results

#### 3.1. X-ray diffraction

The x-ray spectra are shown in Figure 2. Here it can be observed the all the present phases in the monocrystalline and polycrystalline samples corresponds to those reported phases for this material (Austenite  $\beta$  and Martensite $\beta'$ ,  $\gamma_2$ ) [11]. It is obvious that the monocrystal presents only a peak that corresponds to (440) direction; while the hot-rolled polycrystalline sample presents a preferential orientation in (111) and (220) directions; this confirms the existence of global crystallographic texture in the polycrystalline sample.

This result also confirmed the possibility to get the direct transformation by stress (Austenitic-Martensitic); in other words the superelastic effect in this alloy will be observed when the stress-induced martensitic transformation appears during the mechanical test. The  $\beta$  phase or austenite phase is a supercell  $DO_{19}$  wich lattice has a higher order of symmetry than  $\beta'$  martensite phase; this martensite is also known as 18R martensite. The lattice correspondence between martensite and austenite was reported by Zhu et al [30]. In this transformation more than one martensite variant can be induced from one austenite. In addition it has to be pointed out than martensite variants have identical crystal lattice but they can appear in different orientation. The relationship of microstructures is essential to get a better understanding of the mechanical response of this smart material. Once the x-ray analysis confirmed the existence of monocrystalline and polycrystalline samples, the differential screw calorimetric studies were done.

#### 3.2. Differential screw calorimetric analysis

The transformation temperatures  $M_s$ ,  $M_f$ ,  $A_s$ ,  $A_f$ , and the difference  $M_s-M_f$ ,  $A_f-A_s$  are considered as critical factors in characterizing shape memory behavior. There is a strong dependence between transformation temperatures and the alloy's composition and its processing, this is based on microstructural defects, degree of order in the parent phase, and grain size of the parent phase. The mentioned factors can modify the transformation temperatures by several degrees. When the martensitic transformation takes place,

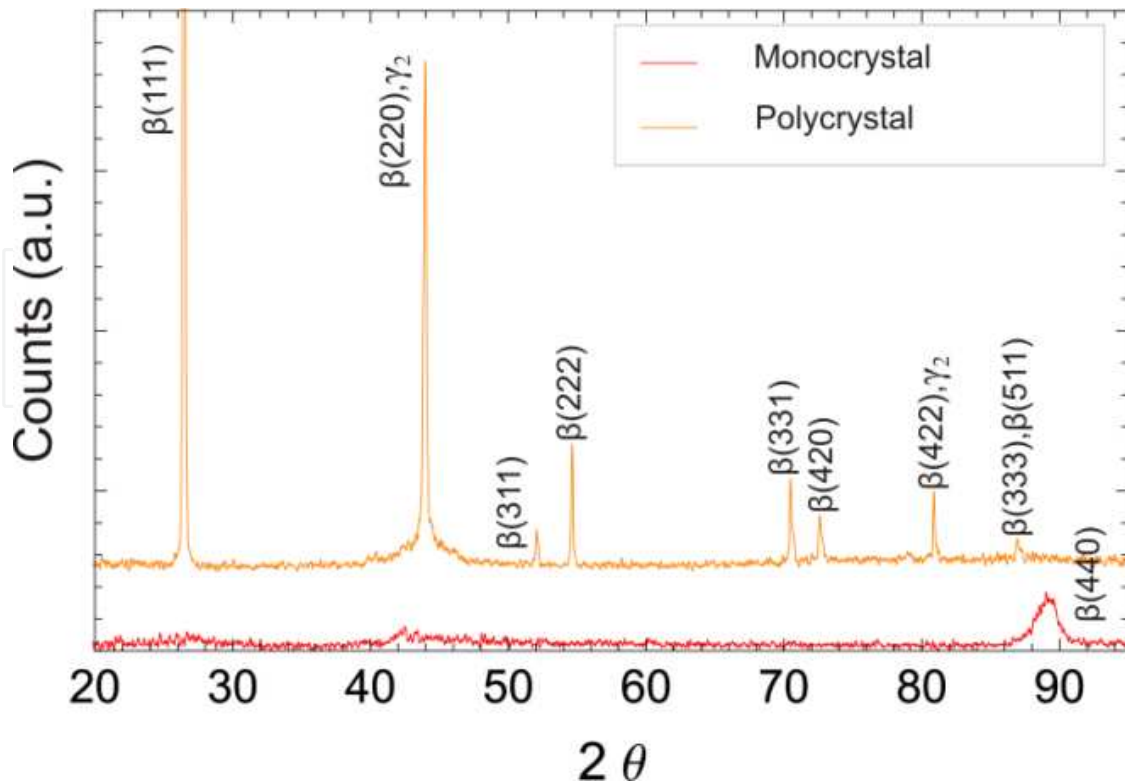


**Figure 2.** X-ray spectra for mono and polycrystalline samples of CuAlBe shape memory alloy

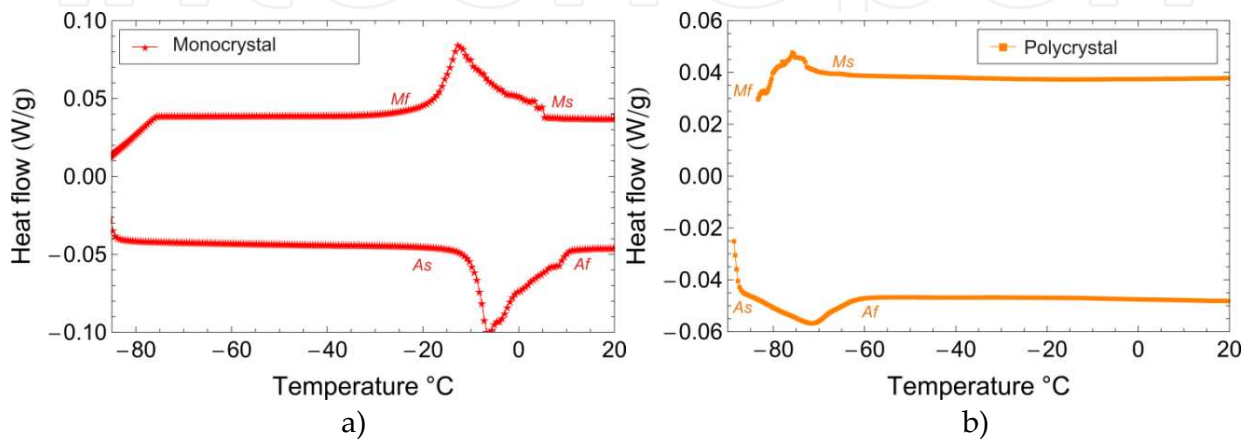
numerous physical properties are modified. During the transformation, a latent heat associated with the transformation is absorbed or released based on the transformation direction. The forward, austenite- to-martensite (A-M) transformation is accompanied by the release of heat corresponding to a change in the transformation enthalpy (exothermic phase transformation). The reverse, martensite-to-austenite (M-A) transformation is an endothermic phase transformation accompanied by absorption of thermal energy. For a given temperature, the amount of heat is proportional to the volume fraction of the transformed material. The two phases also have different resistance due to their different crystallographic structures, so the phase transformation is associated with a change in the electrical resistivity [31].

Figure 3 shows the DSC curves for both kind of samples mono and polycrystal. In this figure can be realized those discontinuities in the heat flow *vs.* temperature curve which corresponds to exothermic reaction during the direct transformation (Austenite to Martensite phase change); additionally the inverse transformation (Martensite to Austenite phase change) is located in the peak that reveals an endothermic reaction. These peaks show the four critical temperatures of transformation in these smart materials. The temperatures were labeled in figure 3 as follows:  $M_s$  corresponds to the beginning of the martensitic transformation;  $M_f$  indicates the end of martensitic transformation. In the same way  $A_s$  and  $A_f$  indicate the start and the end of the inverse transformation. All these temperatures were determined at 10% and 90% of the peak's areas that defines each transformation; they were found using the Universal Analysis 2000 software of TA Instrument. The critical temperatures were summarized in table 1.

Temperatures (°C)	Monocrystal	Hot-rolled Polycrystal
$M_s$	0	-69
$M_f$	-18	-82
$A_s$	-8	-81
$A_f$	5	-66

**Table 1.** Critical temperatures of transformation of CuAlBe system.

After X-ray analysis and DSC studies, the samples were prepared to observe the microstructure of the mono and polycrystalline samples under bending.



**Figure 3.** Calorimetric analysis to determine the four critical temperatures that defines the shape memory effect in the CuAlBe alloy. a) Monocrystal Sample and b) Hot-rolled Polycrystal Sample

Monocrystalline and polycrystalline samples of CuAlBe were tested in 3-point bending. According to the experimental setup showed in Figure 1, the samples were focused with the optical microscope coupled to the CCD camera at the center of the sample ( $l/2$ ); where  $l$  represents the support span. In order to observe the stress-induced martensitic transformation through the regions of interest, the samples were previously polished and chemically etched to reveal the microstructure of each sample (Figure 4). All tested specimens were metallographically prepared and chemically etched with a solution of ferric chloride (2g  $FeCl_3$  + 95 ml Ethanol + 2ml HCl) before the mechanical test.

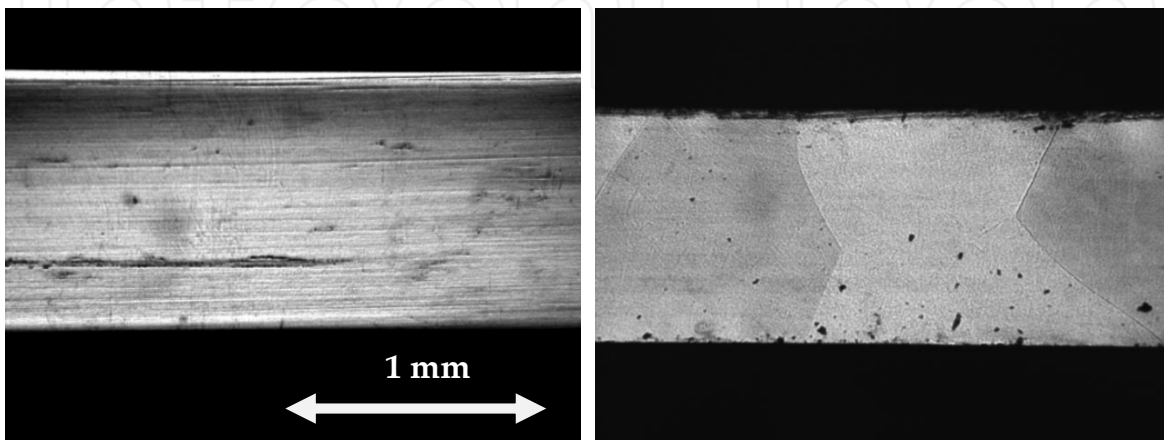


**Figure 4.** Microstructural details of CuAlBe samples in austenitic phase: a) Monocrystal and b) Polycrystal



The Figure 4(a) shows the monocrystal; here it is evident that there are not any grain boundaries while Figure 4(b) shows four grains in a serial arrangement. These two images were taken at the same loading conditions. It is clear that the polycrystal is a little bit thinner than the monocrystal. The thicknesses were 0.9 and 0.7 mm for monocrystal and polycrystal respectively.

### 3.3. Mechanical behavior under 3-point bending

From the 3-point bending test, the force *vs.* neutral axis displacement curves for monocrystal and polycrystal were obtained (Figure. 5). In the case of monocrystal is observed the typical reversible hysteretic loop with a second slope close to zero. The polycrystal showed the same reversible hysteretic loop but the second slope was higher than monocrystal's second slope; as it was expected. This is due to the transformational deformation that is directly associated to stress-induced martensitic transformation, which depends on the applied force direction and the crystals orientations. Now taking in to account the  $M_s$  temperature for monocrystal and polycrystal and the equation of Clausius Clappeyron  $\sigma_c = 1.97MPa(T - M_s)$  which relates the  $M_s$  with the critical transformation stress  $\sigma_c$ , this transformation stress can be easily calculated considering that  $T$  corresponds to the test temperature 20°C; furthermore the critical stresses were around 175 and 40 MPa for polycrystal and monocrystal respectively. This last result is good agreement with the stress transformation values for label B and E in the stress *vs.* neutral axis displacement curve for both samples.

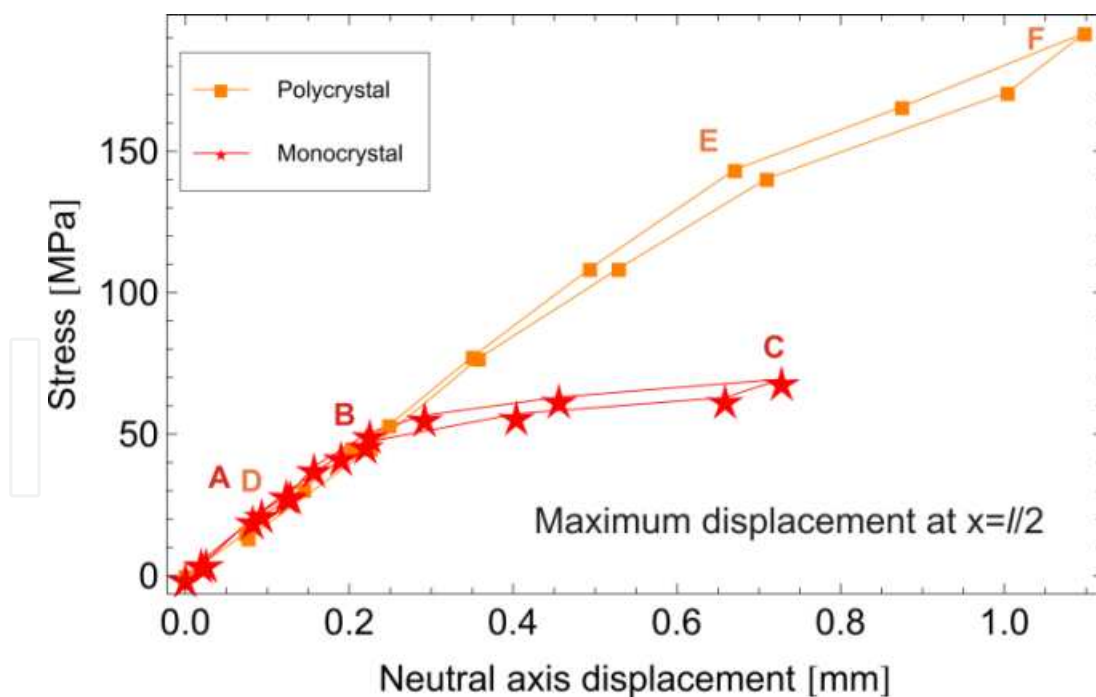


**Figure 5.** Force vs. Neutral axis displacement curves obtained from 3-point bending arrangement

The Figure 5 shows six labels that indicate the associated images in both cases monocrystal and polycrystal samples; the monocrystal images correspond from letter A to C and polycrystal from D to F. This six labels match with the images presented in Figure 6. These

are labeled with the same letters for each case. As it can be observed, the images from A to C showed the austenitic phase (Figure 6A), the beginning of martensitic transformation (Figure 6B) and almost a total martensitic state for the monocrystal under bending (Figure 6C). The polycrystalline sample showed the austenitic phase in all grains (Figure 6D), then the martensitic plates appear in tension and some martensitic plates in compression almost simultaneously (Figure 6E); finally the image (Figure 6F) shows the central region plenty of martensitic plates. It has to be pointed out, that the martensitic plates in the monocrystal sample grow first up in compression and subsequently in tension; in the polycrystalline case happened the opposite.

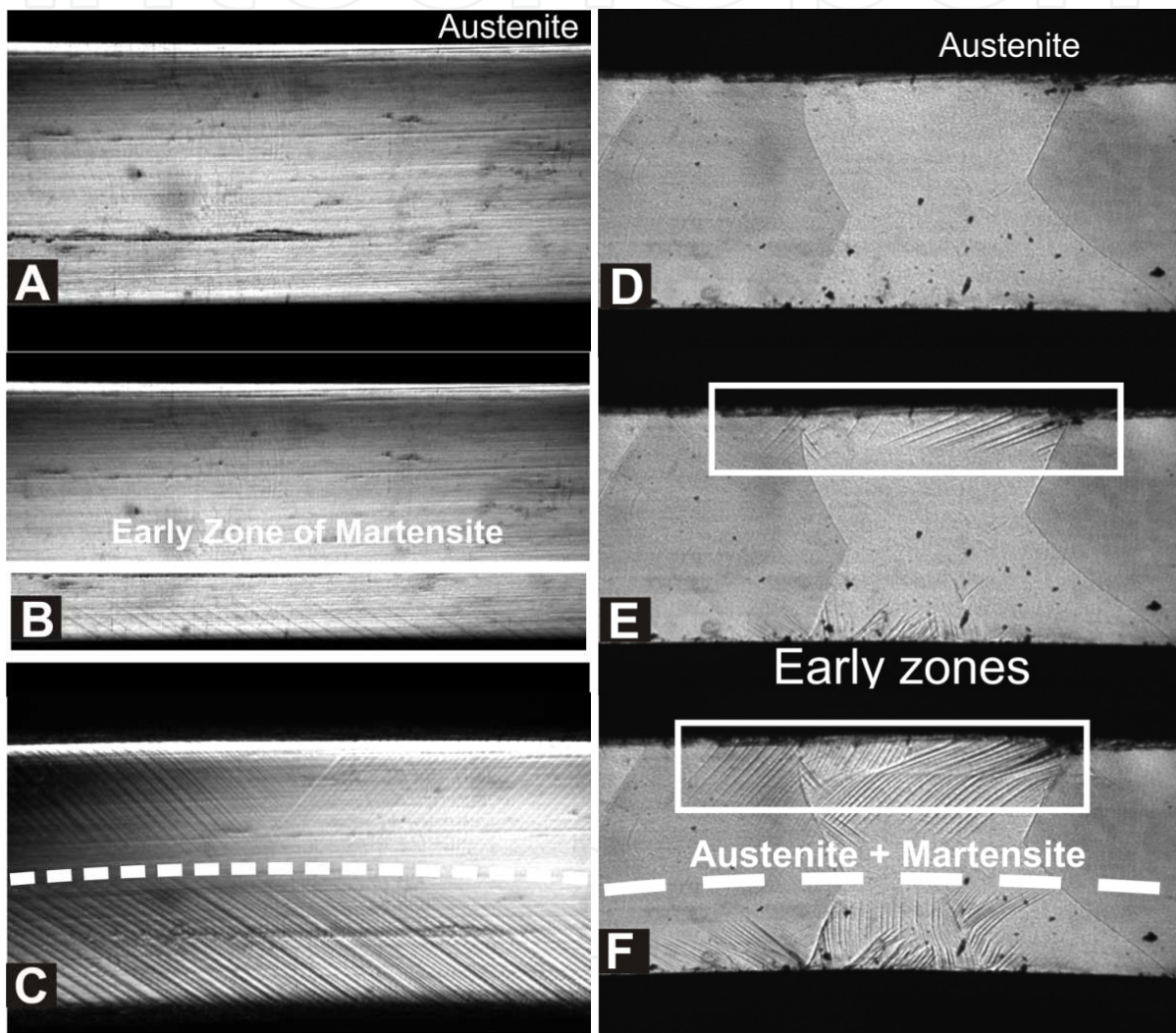


**Figure 6.** Mono and polycrystalline samples of CuAlBe under 3 point bending: a. Monocrystalline austenitic phase; b. Beginning of the martensitic transformation; c. Almost a total martensitic state for the monocrystal under bending; d. Austenitic phase in the polycrystal; e. Growth of the martensite plates in tension and compression; f. Several variants of martensite appear in the same grain

Another interesting observation was about the martensitic variants that grew up in both cases. The monocrystalline sample showed two variants according to the established angles respect to the horizontal line. In tension appeared a variant with two equivalent directions;

at left hand this variant was around  $45^\circ$  and at right hand  $48^\circ$ . In compression the stress-induced martensitic plates showed just a single direction that it was around  $35^\circ$  (Figure 7a). In this case should have appeared two variants close to  $45^\circ$ ; nevertheless, a single variant grew up; it may due to the interaction with the fulcrum.

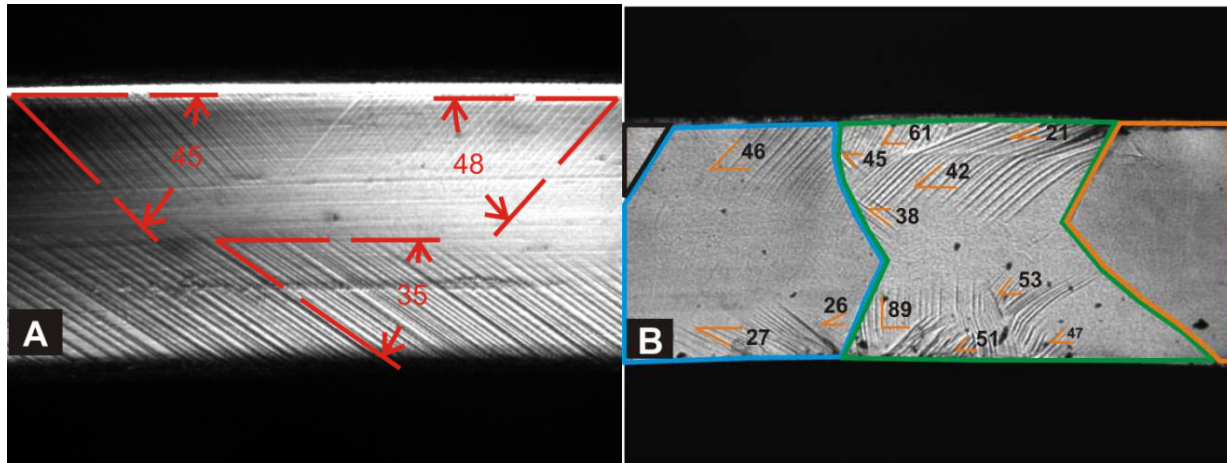


**Figure 7.** Stress-Induced martensitic variants: a) Monocrystal and b) Polycrystal

The Figure 7b shows the polycrystalline case. Here the central grains showed several martensitic variants; the first grain marked in blue showed one martensitic variant around  $46^\circ$  in tension but in compression the same grain showed two variants the first one was around  $27^\circ$  and the second one was around  $26^\circ$  that were different to those in tension; the compression variants are almost perpendicular each other; the grain marked in green is located at the center of the support span. So it is obvious that there are more martensitic plates in this region.

The martensitic plates are in several directions, all of them are close to  $-45^\circ$  or  $45^\circ$ ; nevertheless, there are a couple of variants that appeared in those directions that have less probability to exist according to the applied force direction and the direction of the early plates of martensite. These variants were located at  $89^\circ$  and  $21^\circ$ . It has to be pointed out that these variants appear in the same grain, which has a fixed crystalline orientation. So why do several variants of martensitic plates exist in the same grain? A possible answer is the granular interaction due to the martensitic transformation for the polycrystalline sample. It is clear that in the present work the crystalline orientation of the samples was not measured; however it is possible to infer the growth variants which have more chance to appear, if crystal orientations are guessed.

To identify these variants was used the list of habit planes and directions of Cu-Al-Be system reported by Kaouache et al.[21]. In addition to this list, it was used the procedure proposed by Bucheit et al. to get the surface transformation in single crystals [32]. Using the previous information, the plane stress transformational diagrams for typical crystalline orientations of the Cu-Al-Be in the austenitic phase were calculated in this work. The diagrams present irregular polygonal regions making evident the material anisotropy (Figure 8). This shows the existence of specific variants according to the state of stress (in

typical cases like: tension-tension, tension-compression and compression-compression), habit plane and crystal orientation.

The plane stress transformational diagrams are located among [001], [011] and [-111] directions. It has to be noticed that these diagrams show significant differences between each other according to those guessed crystalline orientations; this means that there will be asymmetry and anisotropy between tension and compression in this material. This result agrees with the images that show the stress-induced martensitic transformation under 3-point bending (Figure 6).

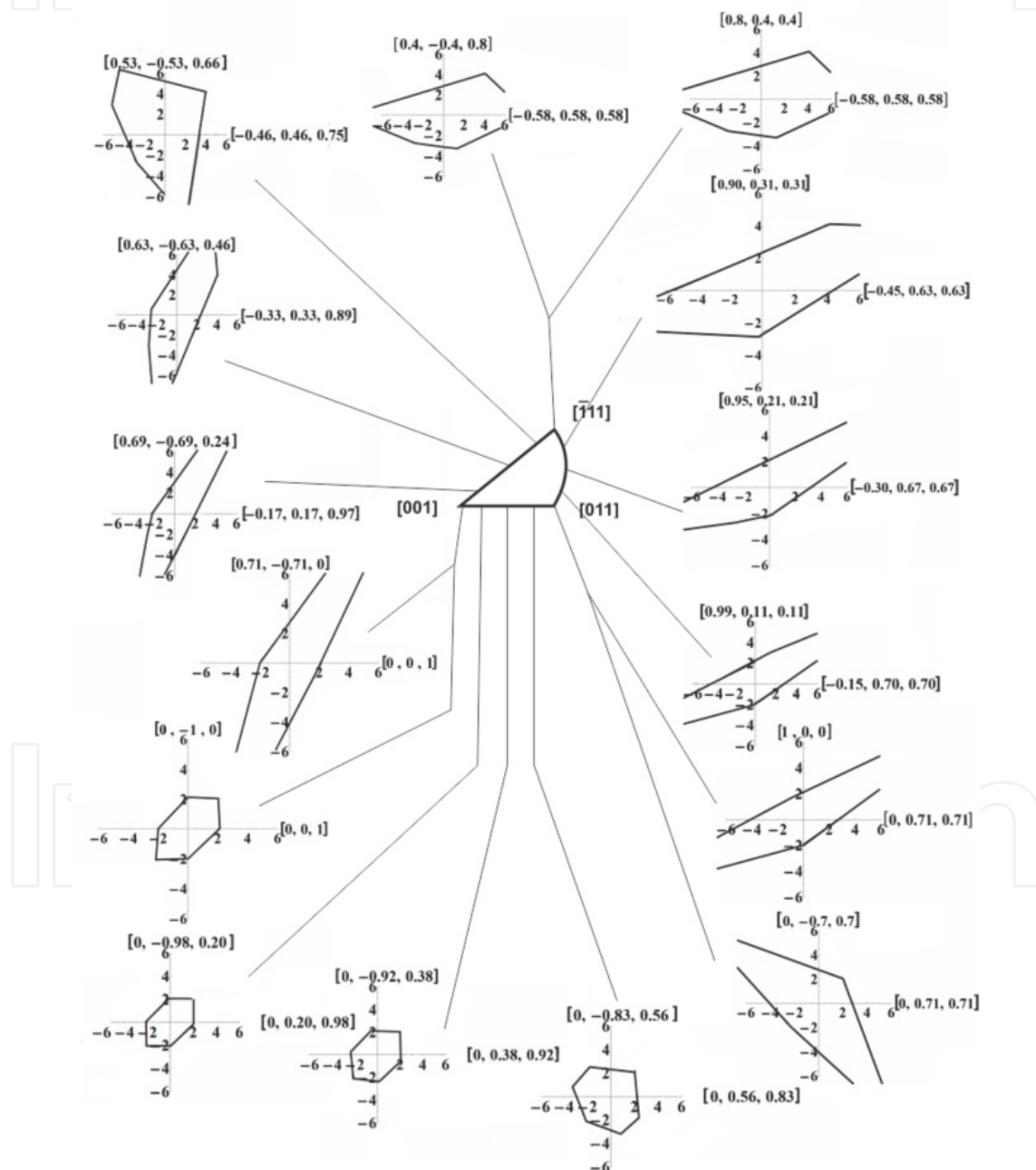


**Figure 8.** Plane stress transformational diagrams for typical crystalline directions of the Cu-Al-Be beta phase associated to different crystalline orientations represented in a stereographic projection.

From Figure 8 were selected four cases where several martensite variants can appear in tension and/or compression under the same applied force direction. The variants were identified according to the calculation proposed by Buccheit et al. for each martensitic variant taking in to account the guessed orientation. In general the diagrams present different variants with the same possibility to appear in accordance with the current state of stress; however, in this case the simple tension and compression cases are shown. These cases are shown in Figure 9; the mentioned variants present exactly the same trace in each circumstance. Here it is shown that several variants can appear because the Schmid Factor is equal for each variant; furthermore they have the same chance to grow up in the crystal. It is important to say that each variant present different mark on the observation surface as it is shown Figure 7.

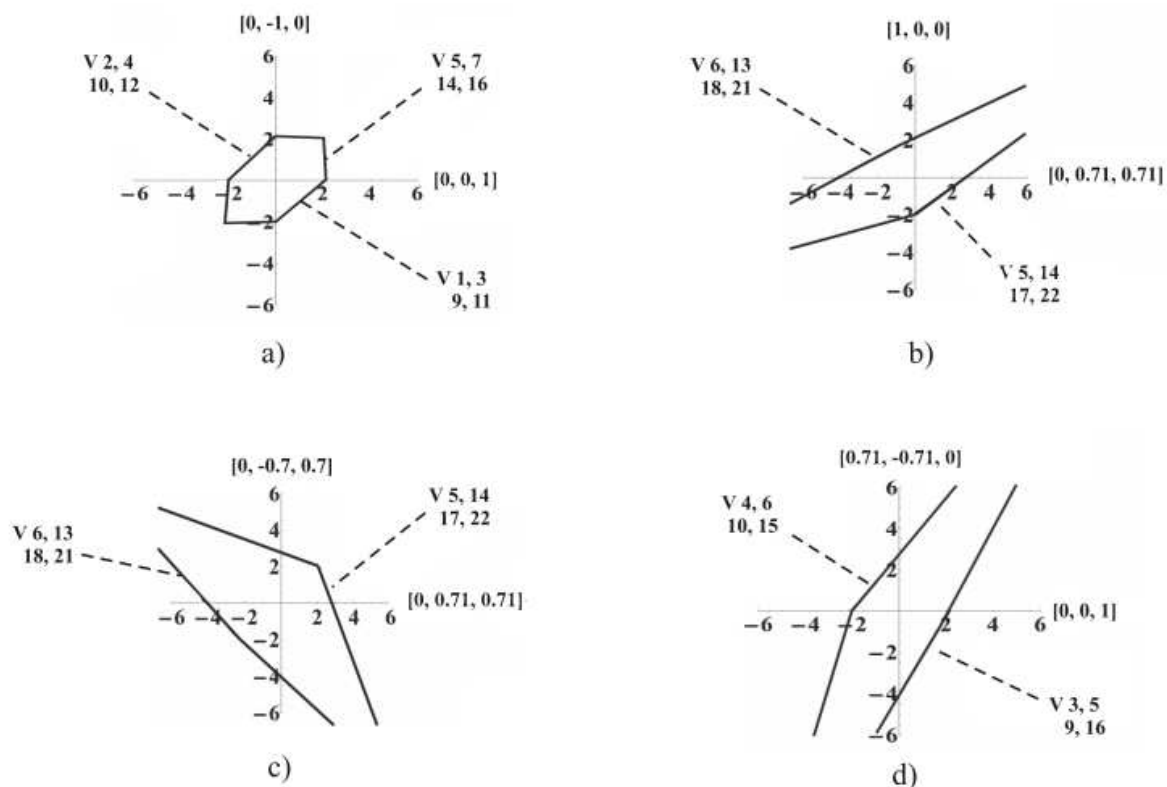


**Figure 9.** Plane stress transformational diagrams of CuAlBe and the Growth of several martensitic variants in a crystal with a fixed crystal orientation under the the same applied force direction. A) this figure shows the growth of 12 possible variants and figure b), c) and d) show four possible variants.

In order to observe the contribution of several martensitic variants to the micromechanical behavior of CuAlBe, digital image correlation was used get the displacement vector fields at different state of stress. The displacement vector fields are showed in Figure 10. Here it can be observed the curvature of the beam under bending.

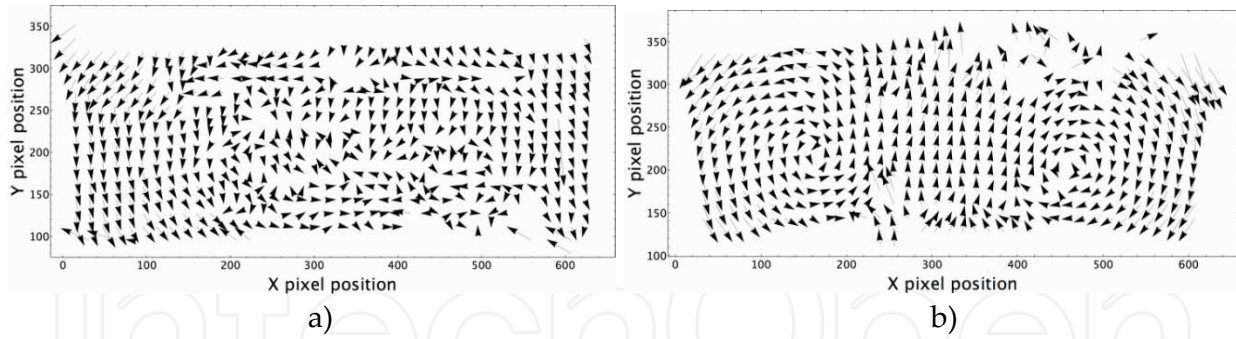


**Figure 10.** Displacement vector fields of samples under 3-point bending: a) Monocrystal and b) Polycrystal.

From these displacement vector fields it is possible to observe that a moment ( $M$ ) is acting in the both sides of the samples. In the polycrystalline case this effect is more evident. Isolating the rotation in “ $xy$ ” plane and the “ $y$ ” displacements was obtained the displacements in the “ $x$ ” direction. These fields were completely overlapped on the corresponding images; they are showed in Figure 11. Here it is possible to observe that the samples are under tension and compression simultaneously.

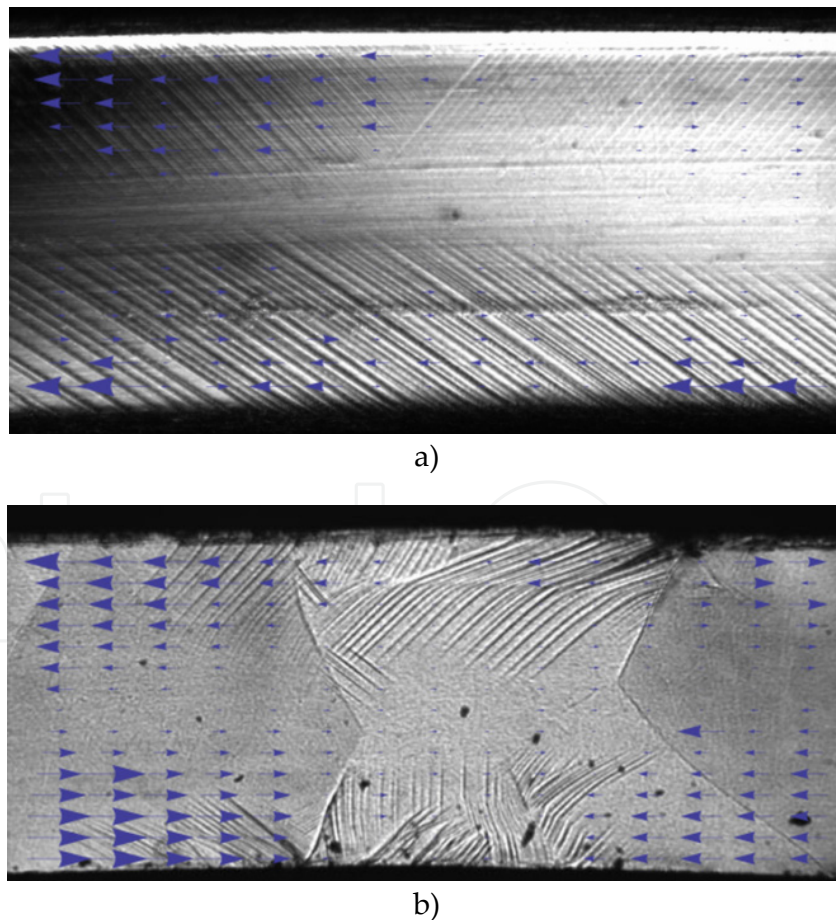


**Figure 11.** Overlapped displacement vector fields on CuAlBe Sample Undergoing 3 point bending: a) Martensitic variants in Monocrystal under tension and compression; b) Martensitic variants in a polycrystal. Martensitic reorientation phenomena is observed.

In both cases, the parts subjected to tension shows the expected “ $x$ ” displacements; nevertheless, the region under compression for the monocrystal did not present the expected displacement vector field. This is due to the growth of a single variant. On the other hand, the region in compression of the polycrystal showed the expected displacement vector field showing compression. In all cases can be observed that the samples of CuAlBe present non-homogeneous behavior but this methodology was able to detect these small contributions in displacement caused by different martensitic variants.

#### 4. Conclusions

This practical methodology was able to observe the micro and macromechanical behavior of Cu-Al 11.2 wt.%-Be 0.6 wt% polycrystal and Cu-Al 11.2 wt.%-Be 0.5 wt% monocrystal shape memory alloy undergoing a stress-induced martensitic transformation by a 3-point bending. The evolution of the martensitic transformation was registered by the CCD and was detected the non-symmetric behavior in tension and compression for both cases mono and polycrystalline samples. The overlapped displacement vector fields show the non-homogenous behavior of monocrystalline and polycrystalline samples of these alloys. This methodology was also able to detect the granular interaction in 2D confined grains; this may due to the interaction between the growth of martensite plates that modified the local state of stress in the grain and their neighbors. It is evident that there is a re-orientation effect of the martensitic phase while the load increases. This interaction provokes the apparition of several martensitic variants in different directions; this was in good agreement with the stress transformation diagrams for CuAlBe alloy.

#### Author details

R.J. Martínez-Fuentes, F.M. Sánchez-Arévalo and G.A. Lara-Rodríguez  
*Instituto de Investigaciones en Materiales, Universidad Nacional Autónoma de México, Cd. Universitaria, México*

F.N. García-Castillo, J. Cortés-Pérez and A. Reyes-Solís  
*Centro Tecnológico Aragón, FES Aragón, Universidad Nacional Autónoma de México, Cd. Nezahualcoyotl Edo. De México, C.P, México*

#### Acknowledgement

The authors wish to thank for the financial support to the DGAPA-UNAM through the IACOD program, project number I1101211 and PAPIIT project number IN111310. The authors are grateful to Esteban Fregoso Israel and Adriana Tejeda Cruz for their technical support.

#### 5. References

- [1] Olson, M.; Cohen, G. B.; Clapp, P.C. On the classification of displacive phase transformations. *Proceedings of the international conference on martensitic transformation. ICOMAT 79, Cambridge-Massachusetts U.S.A. 1979* pp. 1-11.

- [2] Czichos, H. "Adolf Martens and the research of martensite." *Proceedings of the european conference on martensitic transformation in science and technology*. Bochum, Alemania, 1989; pp. 3-14.
- [3] Patoor, E.; Berveiller, M. *Les alliages à mémoire de forme. Technologies de pointe*; Hermes, PARIS, 1990 ; pp 09-63.
- [4] Wayman, C. M.; Duerig, T. M. *An introduction to martensite and shape memory, Engineering Aspects of Shape Memory Alloys*. Butterworth-Heinemann, London (UK), pp. 3-20.
- [5] Oztuka, K.; Wayman, C. M.; Nakay, K.; Sakamoto, H.; Shumizu K. *Acta Metallurgica*, 1976. Vol.24, pp. 207-226.
- [6] Yang, J. H.; Wayman, C. M. *Mater. Charact.* 1992. vol 28, pp. 23-35.
- [7] Yang, J. H.; Wayman, C. M. *Mater. Charact.* 1992.vol. 28, pp. 37-47.
- [8] Higuchi, A.; Suzuki, K.; Matsumoto, Y.; Sugimoto, K.; Komatsu, S.; Nakamura, N. "Shape memory effect in Cu-Al-Be ternary alloy." In: *Proceedings of the international conference on martensitic transformations, ICOMAT 1892*. Leuven, Belgica. pp. 767-772.
- [9] Higuchi, A.; Suzuki, K.; Sugimoto, K.; Nakamura, N. "Thermal stability of Cu-Al- Be shape memory alloy." In: *Proceedings of the international conference on martensitic transformations, ICOMAT 1896*. Nara, Japan. pp. 886-890.
- [10] Belkahla S.; Flores H.; Guenin G. *Mater. Sci. Eng. A-Struct. Mater. Prop. Microstruct. Process.* 1993, A169. p. 119-124.
- [11] Jurado, M.; Castan, T.; Mañosa, L.; Planes, A.; Bassas, J.; Alcobe, X; Morin, M. *Philos. Mag.* 1997, Vol. 5. pp. 1237-1250.
- [12] Hautcoeur, A.; Eberhardy, A.; Patoor, E.; Berveiller M. "Thermomechanical behavior of monocrystalline Cu-Al-Be shape memory alloys and determination of the metastable phase diagram." *Journal de physique IV. Colloque C2, supplément au Journal de Physique III*.1995,Vol. 5. pp. c2-459 to c2-464.
- [13] Siredey, N.; Eberhardt, A. *Mater. Sci. Eng. A-Struct. Mater. Prop. Microstruct. Process..* 2000, A290, pp. 171-179.
- [14] Balo, N.; Ceylan, M.; Aksoy, M. *Mater. Sci. Eng. A-Struct. Mater. Prop. Microstruct. Process.* 2001, A311, pp. 151-156.
- [15] Balo, N.; Ceylan M. *J. Mater. Process. Technol.* 2002 Vol. 124. pp. 200-208.
- [16] Pinh Zhang, Aibin Ma., Sheng Lu, Guanguo Liu, Pinghua Lin, Jinghua Jiang, Chenglin Chu. Effect of grain refinement on the mechanical properties of Cu-Al-Be-B shape memory alloy. *Materials and Design*. 2011. Vol. 32. Pp. 348-352.
- [17] C de Albuquerque V. H. A de melo T. A. Ferreira D. Mediros R. Tavares J. M. Evaluation of grain refiners influence on the mechanical properties in a CuAlBe shape memory alloy by ultrasonic and mechanical tensile testing. *Materials and Design*. 2010. Vol.31. Pp.3275-3281.
- [18] Bouvet C.; Calloch S.; Lexcellent, C. *Transactions of ASME*. 2002,Vol 124. pp.112-124.
- [19] Chevalier, L.; Calloch, S.; Hild, F.; Marco, Y. *Eur. J. Mech. A/Solids*. 2001, vol. 20. pp. 169-187.
- [20] Kaouache, B.; Berveiller, S.; Inal, K.; Eberhardt, A.; Patoor, E. *Mater. Sci. Eng. A-Struct. Mater. Prop. Microstruct. Process.* 2004, A378. pp. 232-237.



- [21] Kaouache, B.; Inal, K.; Berveiller, S.; Eberhardt, A.; Patoor, E. *Mater. Sci. Eng. A-Struct. Mater. Prop. Microstruct. Process.* 2006, A 438-444. pp. 773-778.
- [22] Siridey, N.; Patoor, E.; Berveiller, M.; Eberhardt, A. *Int. J. Solids Struct.* 1999, Vol. 36 pp. 4289-4315.
- [23] Sánchez, F. M.; Pulos, G. *Materials science Forum.* 2006, Vol. 509. pp. 87-92.
- [24] Sánchez-Arévalo, F. M.; Pulos, G. *Mater. Charact.* 2008, Vol. 59. Issue 11. pp. 1572-1579.
- [25] Merzouki T., Collar C., Bourgeois N., Zineb T. B., Meraghni F. 2010. *Mechanics of Materials* Vol. 42 pp. 72-95.
- [26] Bourgeois N., Meraghni F., Zineb T. B. 2010. *Physics Procedia.* Vol. 10 pp. 4-10
- [27] Willert C. E., Gharib M., 1991, *Experiments in fluids.* Vol. 10. pp. 181-193.
- [28] Chu T. C., Ranson W. F., Sutton M.A., Peters W.H. 1985. "Applications of digital correlation techniques to experimental mechanics". *Experimental Mechanics.* 25(3). pp. 232-244.
- [29] Sánchez-Arévalo, F.M., García-Fernández, T., Pulos, G., Villagrán- Muniz, M., 2009. Use of digital speckle patten correlation for strain measurement in a CuAlBe shape memory alloy. *Mater. Charact.* 60, 775–782.
- [30] Zhu J. J., Liew K.M. 2003. Description of deformation in shape memory alloys from DO3 austenite to 18R Martensite by group theory. *Acta Materialia* 51, 2443-2456.
- [31] Patoor E., Lagoudas D. C. Entchev P. B, Brinson, C. Gao X. 2006. Shape memory alloy, Part 1: General properties and modeling of single Crystals. *Mechanics of Materials*, 38, 391-429
- [32] Buchheit T. E. Wert J.A. 1994. Modeling the effects of stress state and crystal orientation on the stress-induced Transformation of NiTi single crystals. *Metallurgical and Materials Transactions A.* 25,283-238.